Supporting information for Cost-Effective Approach for Atmospheric Accretion Reactions: Case of Peroxy Radical Addition to Isoprene

Dominika Pasik, Siddharth Iyer, and Nanna Myllys

CREST Conformational Sampling

Table S1 presents the number of initial CREST conformers at the xTB level found by using different TS search approaches. Approach 1 produces initial product structures for which relaxed potential energy surface scan at the DFT level will be performed and Approach 2 leads initial TS structures which are further optimized and frequencies are calculated at the DFT level.

Table S1: Number of initial conformers found in CREST conformational search in both approaches.

	Approach 1	Approach 2
me-1	26	32
me-2	32	34
me-3	37	30
me-4	44	25
et-1	89	86
et-2	69	38
et-3	117	52
et-4	130	91
p-1.1	261	124
p-1.2	156	76
p-1.3	351	85
p-1.4	397	165
p-2.1	104	73
p-2.2	91	41
p-2.3	130	71
p-2.4	127	76

Density Functional Theory data

Table S2 shows the zero-point energy corrected barrier heights for accretion reaction found by using the Approach 1.

Table S2: DFT energy barriers (kcal/mol) for the studied reactions calculated with using ωB97X-D with three different basis sets.

Approach 1	6-31+G*	Def2TZVPP	aug-cc-pVTZ
me-1	6.66	7.95	8.37
me-2	14.39	16.81	16.30
me-3	15.54	18.12	17.39
me-4	7.47	9.24	9.20
et-1	6.46	8.28	8.15
et-2	14.54	16.52	16.32
et-3	14.57	16.36	16.18
et-4	7.05	8.87	8.74
p-1.1	6.10	7.93	7.76
p-1.2	13.97	15.99	15.79
p-1.3	16.25	17.99	17.80
p-1.4	6.67	8.51	8.30
p-2.1	6.44	8.26	8.11
p-2.2	14.75	16.71	16.55
p-2.3	15.45	17.48	17.26
p-2.4	7.10	8.93	8.78

Table S3 presents the zero-point energy corrected accretion reaction energies found by using Approach 1 and Approach 2.

Table S3: Reaction energies (kcal/mol) calculated on ωB97X-D/6-31+G* level of theory.

	Approach 1	Approach 2
me-1	−14.98	−15.04
me-2	2.43	3.07
me-3	1.52	2.41
me-4	−12.88	−12.87
et-1	−15.05	−14.97
et-2	2.43	3.24
et-3	0.94	2.52
et-4	−11.81	−12.88
p-1.1	−15.41	−15.12
p-1.2	1.98	2.98
p-1.3	0.47	2.24
p-1.4	−13.34	−13.33
p-2.1	−14.81	−14.81
p-2.2	2.65	3.55
p-2.3	1.24	2.82
p-2.4	−12.75	−12.75

Figure S1 shows geometrical structures of lowest energy accretion reaction products of isoprene and methyl, ethyl, 1-propyl and 2-propyl peroxy radicals, respectively (pathway 2). Structural similarities are observed for successive radicals belonging to the same homologous series (see Figure S1).

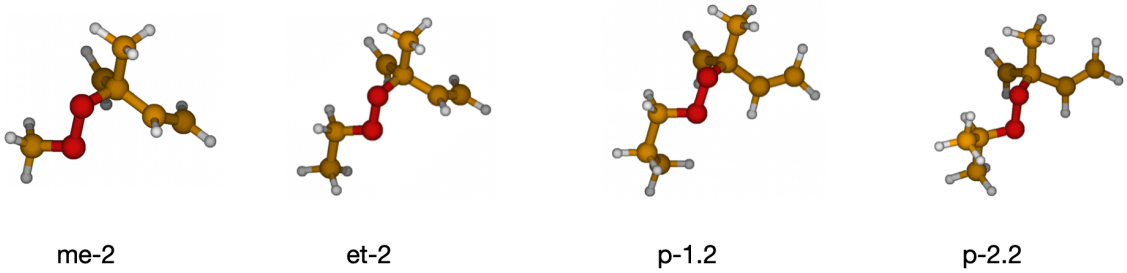

Figure S1: Structures of accretion reaction products of isoprene with methyl, ethyl, 1-propyl, 2-propyl radicals, respectively (pathway 2).

Coupled-Cluster data

The barrier heights obtained using the DLPNO-CCSD(T)/aug-cc-pVDZ method on the top of any of the three DFT structures, are underestimated compared to the more accurate DLPNO-CCSD(T)/aug-cc-pVTZ and CCSD(T)-F12/cc-pVDZ-F12 methods. On the other hand, the differences in barrier heights computed at the DLPNO-CCSD(T)/aug-cc-pVTZ and CCSD(T)-F12/cc-pVDZ-F12 are marginal. As the DLPNO method is computationally much more efficient (linear scaling) than the canonical coupled cluster method (scaling to the seventh power), it can be applied even for large reaction systems sizes. Mean absolute errors of all DFT and CC//DFT barrier energies compared to the most accurate F12/VDZ//DFT/aug-cc-pVTZ values are presented in Figure S2.

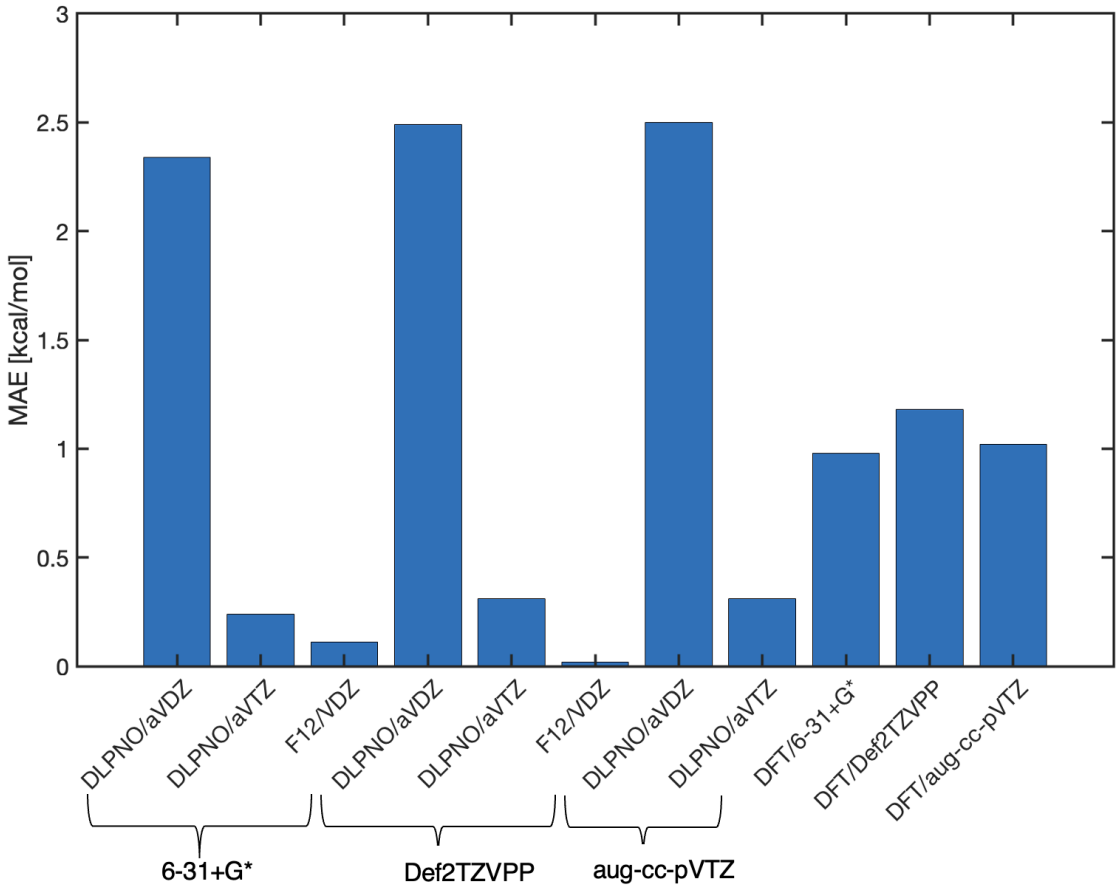

Figure S2: Calculated MAE [kcal/mol] for all methods and basis sets (reference CCSD(T)-F12/cc-VDZ-F12//ωB97X-D/aug-cc-pVTZ)

Due to the fact that it is not possible to compare absolute energy values obtained from calculations using different methods, the values in the Table S4 represent the energy differences of a given conformer relative to the lowest energy structure. As evident from the data presented in Table S4, the results are consistent across all functional basis sets. Assuming that the most reliable values are provided by the optimization with the ωB97xD/aug-cc-pVTZ method and single point energy correction with canonical CCSD(T)-F12/cc-pVDZ-F12 level, it can be observed that in all cases the trend is correct and the calculations indicate that the lowest-energy conformer corresponds to pathway 1. The energy barrier in pathway 4 has only slightly higher energy (0.37–0.74 kcal/mol) than in pathway 1, whereas the barriers in pathways 2 and 3 exhibit significantly higher (5–6 kcal/mol) energy. The results also confirm the pattern obtained by DFT methods: among all structures, the energetically lowest ones are those derived from pathways 1 and 4.

Table S4: Relative energies (kcal/mol) of investigated structures calculated at different CC//DFT levels.

		ωB97X-D/6-31+G*	
Approach 2	DLPNO/aVDZ	DLPNO/aVTZ	F12/VDZ
me-1	0.00	0.00	0.00
me-2	4.69	5.25	5.45
me-3	6.24	6.52	6.71
me-4	0.65	0.59	0.73
et-1	0.00	0.00	0.00
et-2	5.28	5.67	5.78
et-3	6.43	6.48	6.48
et-4	0.38	0.48	0.61
p-1.1	0.00	0.00	0.00
p-1.2	5.18	5.61	5.68
p-1.3	6.32	6.45	6.35
p-1.4	0.38	0.51	0.65
p-2.1	0.00	0.00	0.00
p-2.2	5.65	5.97	6.01
p-2.3	6.78	6.74	6.68
p-2.4	0.49	0.56	0.67
		ωB97X-D/Def2TZVPP	
	DLPNO/aVDZ	DLPNO/aVTZ	F12/VDZ
me-1	0.00	0.00	0.00
me-2	4.75	5.41	5.56
me-3	6.21	6.64	6.76
me-4	0.63	0.66	0.74
et-1	0.00	0.00	0.00
et-2	5.26	5.65	5.74
et-3	6.48	6.52	6.50
et-4	0.37	0.44	0.56
p-1.1	0.00	0.00	0.00
p-1.2	5.18	5.58	5.63
p-1.3	6.36	6.51	6.39
p-1.4	0.41	0.55	0.67
p-2.1	0.00	0.00	0.00
p-2.2	5.56	5.88	5.94
p-2.3	6.78	6.68	6.63
p-2.4	0.50	0.55	0.65
		ωB97X-D/aug-cc-pVTZ	
	DLPNO/aVDZ	DLPNO/aVTZ	F12/VDZ
me-1	0.00	0.00	0.00
me-2	4.74	5.41	5.56
me-3	6.22	6.65	6.77
me-4	0.60	0.64	0.72
et-1	0.00	0.00	0.00
et-2	5.24	5.62	5.72
et-3	6.44	6.47	6.45
et-4	0.38	0.45	0.56
p-1.1	0.00	0.00	0.00
p-1.2	5.23	5.63	5.69
p-1.3	6.39	6.53	6.41
p-1.4	0.43	0.56	0.68
p-2.1	0.00	0.00	0.00
p-2.2	5.58	5.85	5.93
p-2.3	6.78	6.67	6.63
p-2.4	0.50	0.55	0.65

For the pathway showing the lowest energy barriers for the investigated reactions, and thus the most probable pathway, a comprehensive comparative analysis was conducted between Approach 1 and Approach 2. For Approach 1, unique conformers were identified for each system (me-1, et-1, p1-1, p2-1), and their corresponding transition states were manually located. Subsequently, structures were optimized on the ωB97X-D/6-31+G* level of theory. Reaction rate coefficients were calculated with MC-TST and LC-TST equations. The results for both approaches are presented in the Table S5.

Table S5: Bimolecular reaction rate coefficient values for investigated systems (pathway 1) for structures form Approach 1 and Approach 2.

Approach 1	LC-TST	MC-TST	Energy barrier [kcal/mol]	# of unique conformers
me-1	1.22E-21	2.20E-21	8.34	5
et-1	1.85E-21	7.93E-22	7.87	11
p-1.1	1.40E-21	3.32E-21	7.60	41
p-2.1	1.66E-21	2.17E-21	7.72	16
Approach 2				
me-1	1.22E-21	2.30E-21	8.34	10
et-1	1.85E-21	1.10E-21	7.87	25
p-1.1	2.01E-21	3.37E-21	7.50	54
p-2.1	1.66E-21	2.18E-21	7.72	19

For each system, the MC-TST reaction rate coefficients calculated for Approach 2 yield higher (and thus better) value.